Breakdown Strength and Dielectric Recovery in a High Pressure Supercritical Nitrogen Switch

J. Zhang, E. J. M. van Heesch, F. J. C. M. Beckers, A. J. M. Pemen
Eindhoven University of Technology
Department of Electrical Engineering
P.O.Box 513, Eindhoven, 5600 MB, the Netherlands

R. P. P. Smeets
DNV GL - Energy
KEMA Laboratories
Arnhem, the Netherlands

T. Namihira
Kumamoto University
Graduate School of Science and Technology
Kumamoto, 860-8555, Japan

A. H. Markosyan[1,2]
[1.] University of Michigan, Departement of Electrical Engineering and Computer Science,
1301 Beal Ave., Ann Arbor, Michigan 48109-2122, USA
[2.] Centrum voor Wiskunde en Informatica (CWI), P.O. Box 94079, 1090 GB
Amsterdam, the Netherlands

ABSTRACT

Fast and repetitive switching in high-power circuits is a challenging task where the ultimate solutions still have to be found. We proposed a new approach. Supercritical fluids (SCFs) combine favorable properties of liquids - insulation strength, thermal behavior, and gases - self healing, high fluidity, and absence of vapor bubbles. That's why we start investigating the subject of plasma switches in SC media. First results indicate excellent switch recovery and very high insulation strength. We present the design of a SCF insulated switch (SC switch). Breakdown strength of the SCF is investigated and found to be high in comparison with most of the solid insulating media. The dielectric recovery inside the SC N_2 switch is tested under a repetitive 30 kV, 200 ns pulse voltage at repetition rate up to 5 kHz. The recovery breakdown voltage across the SC switch achieves 80 % within 200 μs. The current interruption capability of SC N_2 is investigated experimentally in a synthetic circuit generating a high-frequency arc of several hundreds of amperes and a transient recovery voltage of hundreds of volts. The results show that a SC N_2 switch with fixed electrodes and an inter-electrode distance of mm range can successfully interrupt this current at approximately 2 ms after arc initiation.

Index Terms - **Pulsed power, high-voltage switch, supercritical fluids, plasma, high-pressure plasma, breakdown voltage, dielectric recovery, arc**

1 INTRODUCTION

SUPERCRITICAL fluids (SCFs), widely researched in chemistry, have recently drawn attention for their potential in the area of electrical switching, due to their combined advantages of liquids and gases. Plasma in SCFs is a quite new research area that covers fundamental researches and applications for a wide area: SC plasma chemistry, SC plasma power switches, and dense planet atmosphere, etc.. Figure 1 gives an overview of the application fields of plasma in SCFs.

Plasma chemistry studies on SCFs mainly focus on the near-critical region, where the properties of the fluid change significantly with a minor variation in pressure or temperature.

Manuscript submitted on 31 October 2014, in final form 20 February 2015, accepted 30 March 2015.

DOI 10.1109/TDEI.2015.005013

Reported applications of plasma chemistry in SCFs are oxidative destruction of toxic waste [1], conversion of organic compounds [2], small scale experiments involving chromatography [3], metal processing such as implantation and deposition [4], etc.. The researches on plasma discharges in SCFs also involve lightning phenomena on extra-terrestrial planets such as Venus where the surface atmosphere is in SC condition due to the temperature and pressure [5].

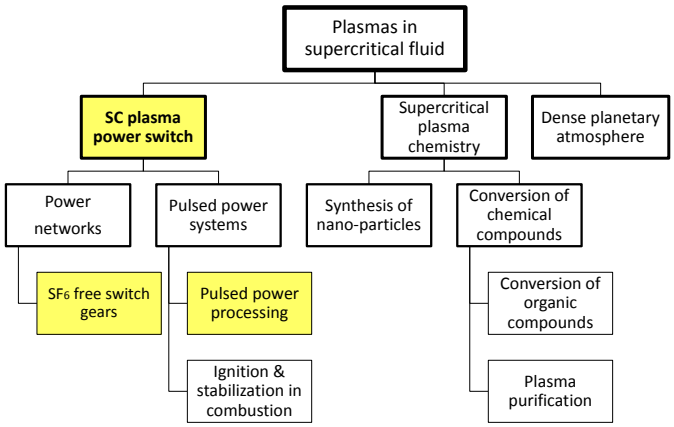

Figure 1. Application area of plasmas in supercritical fluids. The research area of interest in our work is high-lighted.

Circuit breakers in utility power systems protect components and control power flow. High dielectric strength and fast dielectric recovery are vital characteristics. The same criteria are to be met by switches in repetitive pulsed power sources. The historical choice in utility power networks is to apply SF_6. Apart from major technical advantages, this has major disadvantages: it is a strong greenhouse gas, and the degradation products are very toxic. The potential of SCFs in high power switching applications is less explored. The combined advantages of liquids and gases provide the very attractive capability of high breakdown strength and fast dielectric recovery in SCFs. Hence SCFs might be an alternative to SF_6 in circuit breakers in power utility networks. In this work we concentrate on the application of SCFs as insulating media in a repetitive power switch. The arc interruption capability of a SC N_2 switch, as the starting point of the application of SCFs as switching media in circuit breakers, is investigated experimentally in a very initial stage with high-frequency current at low amplitude.

2 SUPERCRITICAL FLUID PROPERTIES

A substance is in the SC state if its pressure and temperature are both above a certain limit, specific for each substance. In the supercritical state the difference between gas and liquid disappears, and no phase separation into bubbles or droplets or a gas phase above a liquid phase can occur. Figure 2 summarizes the relevant properties and behavior related to SCFs.

A comparison of the order of magnitude of the physical properties for common insulating media in the three phases is given as table 1. Density ρ of a SCF is liquid like and the viscosity υ is gas like. Heating a liquid above boiling conditions causes vapor bubbles, while heating a SCF does not cause vapor bubbles. This is the important property for application in high-voltage. Other important advantages for high-voltage application include high heat capacity c_p, high diffusivity D, and high heat conductivity λ. Switching in pulsed power applications requires devices that have quite extreme capabilities: high insulation strength during off mode, low resistance during on mode, large current rating, high voltage rating, fast switching time, allowing high repetition rate switching, fast recovery after switching, low inductance, self-healing medium, long life time, and accepting large overloads. Based on the properties of SCFs, we foresee very good performance of such media for this pulsed power component.

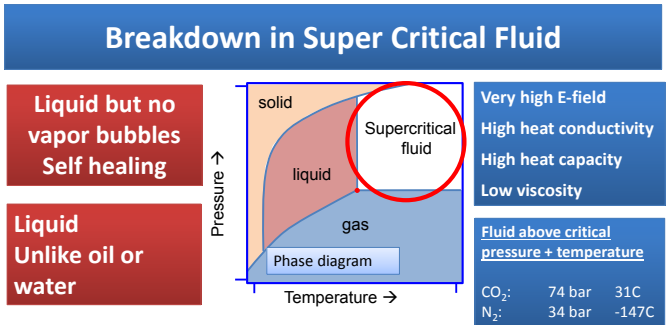

Figure 2. Summary of the relevant properties and behavior related to SCFs. In the middle is the state diagram of a substance, indicating the SC state (red circle).

Table 1. Comparison of the order of magnitude of the properties for common insulating media in gas and liquid, phases and SC N_2. The value of D is the order of magnitude figure for N_2 in range of T = 70 - 500 K, p = 0.1 - 80 MPa.

	ρ [kg/m³]	c_p [10⁶J/m³/deg]	υ [μPa·s]
Gas at STP	1	1	10
SC N_2	100	100	50
Liquid	500	500	100
		λ [10⁻³J/m/s/deg]	D [m²/s]
Gas at STP		20	10 - 300
SC N_2		100	2 - 60
Liquid		200	1 - 2

Recent data about breakdown voltage in SCFs, e.g. SC carbon dioxide, SC argon and SC helium, have proven satisfying dielectric strength of SCFs [6]–[9], while the performance of SCFs in dielectric recovery has rarely been studied. There is no report yet about the arc interruption capability of SCFs.

In our study of switching performance of SCFs, SC N_2 is chosen to be studied for the SC switch, because of its relatively low critical pressure of 3.4 MPa and low critical temperature of 126 K. Experiments with SC N_2 can be performed at room temperature. N_2 is the major component of the Earth's atmosphere, so it has no environmental impact.

3 SC SWITCH AND EXPERIMENTAL SETUP

3.1 SC SWITCH DESIGN

We have designed several SC plasma switches for the experimental investigation of the breakdown strength, dielectric recovery, and arc interruption capability of the SC N_2. An example of the SC switch design is given in figure 3. An aluminum switch house provides sufficient mechanical strength for SCF pressure up to 20 MPa (200 bar); the integration of the capacitor minimizes the stray inductance in the circuit; the adjustable electrode body facilities a variable gap width of 0 - 1.2 mm , with accuracy of ± 0.01 mm ; replaceable heavy duty electrode heads provide change of electrode for erosion investigation; optical windows enable optical observation inside the SC switch; integrated Rogowski coil and capacitive voltage sensor enable high band width current and voltage measurements; the flange on the right attached to the 4-stage transmission line transformer (TLT) [10] is the output connection. To the load it supplies a 4-fold voltage amplification, i.e. 120 kV peak value, facilitating further study of higher voltage SC switch breakdown in the future.

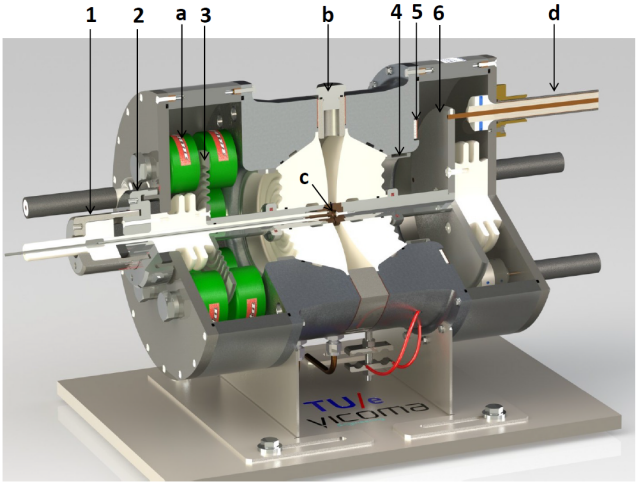

Figure 3. Versatile supercritical medium switch and the schematic of its setup a. integrated capacitor; b. optical sight plug; c. adjustable gap width; d. 4-stage TLT voltage amplifier; 1. Adjusting knob for trigger electrode; 2. Adjusting knob for main electrode; 3. Flexible aluminum disk for gap width adjustment; 4. Rogowski coil; 5. Copper plate for voltage sensor; 6. Stainless steel plate for voltage sensor.

3.2 EXPERIMENTAL SETUP

We have applied various charging circuits, to test the breakdown strength of the SC N_2 switch. The charging circuits generate different voltage impulses, which we classify into three types: fast pulses with charging rate of 2 kV/ns, moderate pulses with charging rate of 2.5 kV/μs, and slow pulses with charging rate of 1.66 kV/ms. The typical waveforms of these voltage impulses are illustrated in Figure 4.

We also implement a repetitive voltage source with repetition rate of up to 5 kHz, to test the dielectric recovery of the SC N_2 switch. A typical voltage waveform measured on the anode of the SC switch under this charging circuit is given in Figure 5. The voltage applied to the switch has a rate of rise of 1 kV/μs and a peak value of 25 - 30 kV.

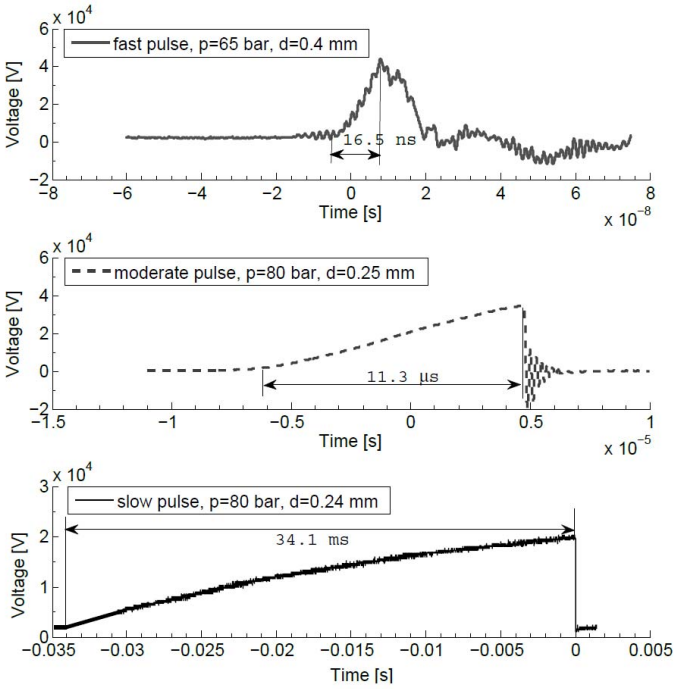

Figure 4. Fast (2 kV/ns), moderate (2.5 kV/μs), and slow (1.66 kV/ms) charging voltage pulses applied to the SC switches.

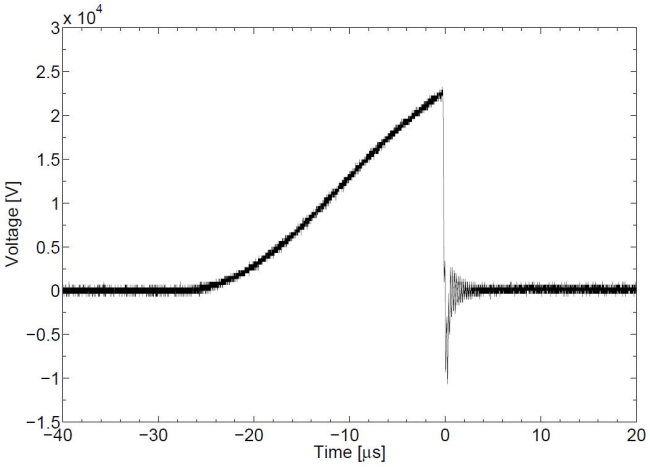

Figure 5. Typical voltage waveform measured on the anode in the SC switch connected to the 5 kHz charging circuit. Gap pressure and gap width: p = 7.5 MPa (75 bar), d = 0.25 mm.

Besides high breakdown strength and fast dielectric recovery capability, arc interruption is the most important property of insulating media in circuit breakers (CB). CBs in power system networks can only interrupt the arc at current zero crossing, and the electrodes must be separated widely enough, in order to quench the arc. In order to study the arc interruption behavior of the SCFs insulated switches, we have designed and manufactured a SC switch with maximum pressure of 20 MPa (200 bar) and an

adjustable gap width in the range of $0.5-5\,\mathrm{mm}$. Since this work is the starting point of the arc interruption study, we made the structure of the switch as simple as possible. Hence, the construction of the SC switch differs considerably from the layout of mechanical CBs in the power system networks: 1) the electrodes in the switch are stationary, while in CBs moving electrodes are applied; 2) the flushing direction in the SC switch is perpendicular to the arc generated in the gap, while in CBs the flushing of insulating media is in an axial direction, parallel to the arc.

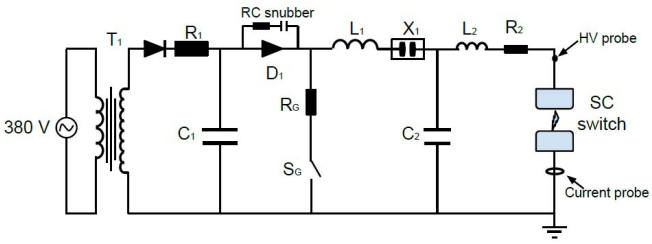

Figure 6. Schematic of the synthetic arc interruption testing circuit for the SC switch.

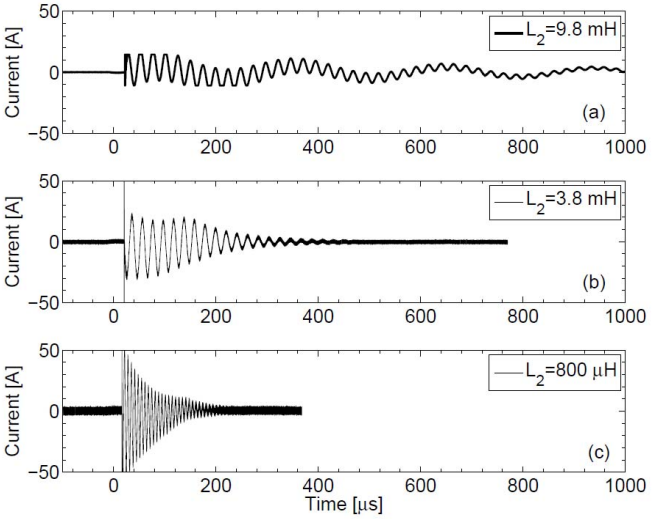

Figure 7. Examples of the measured current through the SC switch with different settings of inductance L_2 in the arc interruption testing, under N_2 pressure of 50 bar and gap width of 0.986 mm.

The arc interruption capability of this SC switch is tested under a synthetic source circuit, illustrated in figure 6. In the circuit the capacitor C_1 is charged by transformer T_1 via a large resistor $R_1 = 120\,\mathrm{M\Omega}$, to a peak voltage up to $50\,\mathrm{kV}$. Diode group D_1 with snubber circuits provides uni-directional energy flow in the circuit. A grounding switch S_G connected with resistor $R_G = 1\,\mathrm{M\Omega}$ discharges the remaining energy in the circuit after the test. Once the air spark gap X_1 (with threshold voltage in the range of $20-40\,\mathrm{kV}$) fires, a capacitor C_2 with value of $C_2 << C_1$ is charged by C_1 via an inductance L_1. When the voltage on C_2 reaches the breakdown voltage of the SC switch, the SC switch breaks down and the current flows through the SC switch, oscillating with a frequency depending on the value of $L_2 - C_2$. The energy stored in C_1 and C_2 is deposited into the SC switch and into the resistor as long as the arc channel in the switch exists.

By choosing the value of C_1 and C_2, we can determine the maximum energy that will be deposited into the SC switch. L_1 determines the rising slope of the voltage applied to the SC switch. The current oscillation frequency, peak amplitude, and damping time constant are controlled by the value of L_2 and R_2. The values of the parameters are $C_1 = 16\,\mathrm{nF}$, $L_1 = 115\,\mathrm{mH}$, $C_2 = 1\,\mathrm{nF}$, $R_2 = 10\,\Omega$, and $L_1 = 800\,\mu\mathrm{H} - 9.8\,\mathrm{mH}$. Examples of the current waveforms with different settings of L_2 are given in figure 7. From the figure it is clear that with a fixed C_2, larger L_2 results in lower oscillation frequency of the arc current and longer duration of the current.

4 EXPERIMENTAL RESULTS

4.1 BREAKDOWN VOLTAGE ANALYSIS

Regarding breakdown voltage increase with the product of pressure and gap width pd, the same trend as in a normal gas is observed in SC N_2. We measured an increasing breakdown electric field as a function of pd under various voltage sources. We have tested two SC switches under three pulsed voltage sources with relatively slow, moderate, and fast voltage rising edges, as seen the example voltage waveforms in figure 4.

In high pressure gases including SCFs, the measured breakdown voltage is found to be lower than the value calculated by the Paschen's law. The possible reasons are: 1) the electron-field emission from the cathode under high density situation [12, 13]; 2) the ionization is enhanced at protrusions on the electrode surface [14]; 3) particles or dusts are responsible for the micro-discharge generated near by the electrodes [14, 15]. Simply calculating the breakdown voltage by Paschen's law using the discharge constant cannot precisely predict the breakdown voltage in high pressure gases. In order to more precisely calculate the breakdown voltage in SCFs, in our work we take the factor of enhanced ionization into consideration. The experimental breakdown voltages in SC N_2 switches are compared with the values calculated from two approaches: I) Paschen's curve calculated from the Townsend breakdown mechanism and II) streamer inception criterion considering enhanced ionization coefficient.

The Paschen's curve in N_2 can be calculated by equation (1). In the equation the constants A and B are dependent on the gas composition: $A = 112.50\,\mathrm{ionization/(kPa\cdot cm)}$, $B = 2737.50\,\mathrm{V/(kPa\cdot cm)}$. The discharge constant K is expressed by equation (2) [16]. The breakdown strength following streamer inception criterion is calculated by assuming a streamer initiating from a small protrusion on the electrode surface. Under a background electric field E_0,

the axial distribution of the electric field has the form of $E(x) = E_0 f(x)$, in which f(x) is the geometric function, depending on the shape of the protrusion. The applied geometry of the protrusion and the value of f(x) can be found in [17]. Under an electric field $E_0 = E_{bd}$, if the streamer criterion [18] given as equation (3) is satisfied at $x_{cr} \approx d$, we say that the streamer can bridge the electrodes hence cause the breakdown of the SC gap. The value of $\ln(N_{cr})$ as a function of the pd value is given in equation (4) [19].

$$V_b = \frac{B \cdot pd}{\ln \frac{A \cdot pd}{K}} \tag{1}$$

$$K = \begin{cases} \dfrac{A}{\exp(2.5819 \times (pd)^{-0.0514})}, & 0.0133 \le \dfrac{pd}{\text{kPa} \cdot \text{cm}} \le 3 \\ \dfrac{A}{\exp(2.4043 \times (pd)^{0.1030})}, & 3 \le \dfrac{pd}{\text{kPa} \cdot \text{cm}} \le 100 \\ \dfrac{A}{\exp(3.8636)}, & 100 \le \dfrac{pd}{\text{kPa} \cdot \text{cm}} \le 1400 \end{cases} \tag{2}$$

$$\int_0^{x_{cr}} \alpha(E(x))dx = \ln(N_{cr}) \tag{3}$$

$$\ln(N_{cr}) = \begin{cases} 13.4 + 1.74 \ln(pd), & 0.2 \le \dfrac{pd}{\text{kPa} \cdot \text{cm}} \le 5 \\ 5.75 - 0.76 \ln(pd), & 5 \le \dfrac{pd}{\text{kPa} \cdot \text{cm}} \le 1000 \end{cases} \tag{4}$$

1 bar = 0.1 MPa. The reduced breakdown field E_{bd} calculated from the simple Paschen's law as well as from the streamer inception criterion with enhanced ionization are plotted in figure 8. The discontinuity of the dashed line in figure 8 is caused by the dependence of $\ln(N_{cr})$ on the value of pd, as shown in equation (4). The measured breakdown strength of SC N_2 switches are plotted in the figure as well. The calculated E_{bd} values are compared with the measurements.

The measured E_{bd} in SC N_2 is as high as 180 kV/mm at $pd = 50\ \text{bar} \cdot \text{mm}$. This is comparable to solid insulating materials which have breakdown strengths reported to be $10 - 150$ kV/mm for our gap width range. In the case of very thin films, some materials have higher breakdown strength (around 400 kV/mm for 40 μm film of Kapton) [20]. From the measurements we can find that in general E_{bd} increases with higher value of pd, but the gain slows down for higher pd values. This observation confirms the description by Cohen [21] in his work on electric strength of highly compressed gases. The scattering of the breakdown strength is larger in SC phase than that in gas phase.

At pd value below 15 bar·mm the measured E_{bd} matches the prediction by Paschen's law. Above this value deviation from Paschens's curve is observed, and the value of E_{bd} tends to saturate from around $pd = 40\ \text{bar} \cdot \text{mm}$ onward. No obvious distinction regarding to the steepness of the voltage sources is observed. Except for $d > 0.6$ mm, the measured E_{bd} does not show much difference at different gap widths. For $pd > 20\ \text{bar} \cdot \text{mm}$ the streamer inception criterion with enhance ionization mechanism gives good prediction of the breakdown strength in SC N_2.

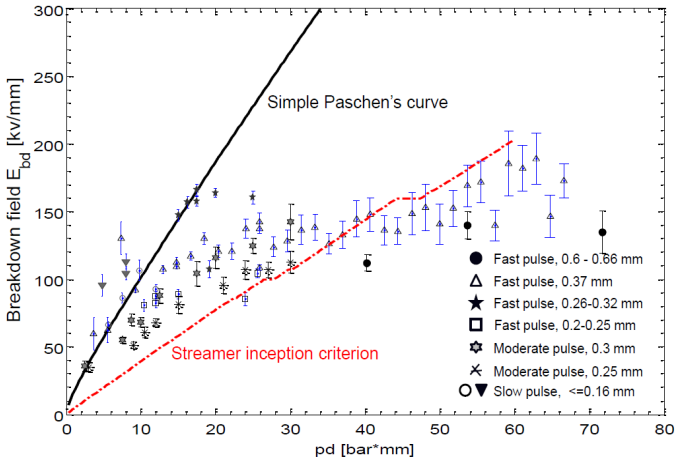

Figure 8. Comparison of the experimental data on the breakdown field E_{bd} in SC N_2 switches with theoretical calculations. Solid line represents Paschen's curve in N_2; dashed line represents the calculated breakdown field following the streamer inception criterion with enhanced ionization on the small protrusion at electrode surface.

4.2 DIELECTRIC RECOVERY ESTIMATION

Due to the gas like high diffusivity, viscosity and liquid like high thermal conductivity, the heat transfer in SCFs is considered to be faster than that in gases. The experimentally observed dielectric recovery time in an air insulated plasma switch is in range of a few to tens of millisecond, depending on the air flushing rate, while from rough prediction by a simple analytic model, the recovery time in SC N_2 is about 1.5 ms at pressure of 150 bar [11].

In the experimental test we measured the recovery of SC N_2 as a function of pd under the 5 kHz in burst mode. We only use pre-fire mode here. Breakdown occurs below the charging voltage of 30 kV. The repetition rate was increased from 5 to 5000 Hz (corresponding to time lag between two succeeding pulses varying between 200 μs and 0.2 s). Figure 9 gives the measured recovery breakdown voltage of the SC N_2 switch at pressures of 30 - 75 bar and gap width of 0.25 mm. Drawing a line from 1 Hz to 5 kHz in figure 9, we estimate that at pressure of e.g. 75 bar, the recovery breakdown voltage at 5 kHz has decreased to ca. 80 % of the cold breakdown value (value at 1 Hz).

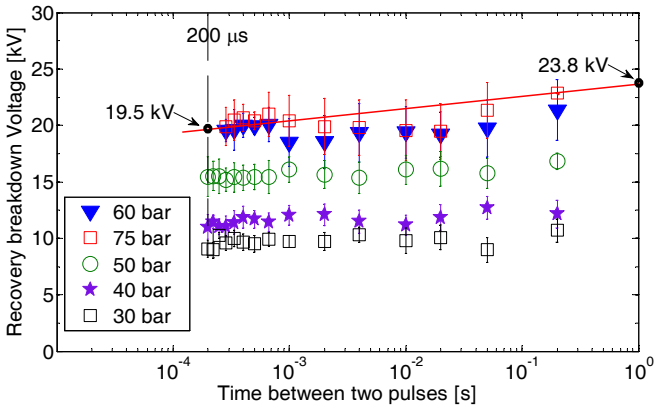

Figure 9. Results from the 1-5000 Hz pulse source: the recovery breakdown voltage of the SC N_2 switch in pre-firing mode as a function of time lag between pulses. The relation with the cold breakdown voltage (= 1 Hz) is estimated by drawing a line from 1 Hz till 5 kHz of the measured data. No SCF flushing is supplied during the experiment.

4.3 ARC INTERRUPTION ANALYSIS

Current and voltage traces in case of successful interruption will be different from the ones in case of continued conduction in the switch. If the SC switch is able to interrupt the current and can recover to a non-conducting state before all the energy in the capacitors is dissipated, the capacitor C_2 will be charged again by C_1. A transient recovery voltage will be observed on the anode of the SC switch. On the other hand, if the SC switch cannot interrupt the current, all the energy in C_1 and C_2 will be deposited into the discharging loop of the switch and C_2 will not be recharged by C_1. The current through the SC switch will decay to zero.

In case of the arc current shown in figure 7(a), a successful interruption was observed at 2 ms after the arc imitation in a gap of d > 1.7 mm, with forced flushing estimated to be 50 Liter/h (corresponding to 2.73 m^3/h at STP). Examples of the arc voltage and arc current under the situation of successful arc interruption are shown in figure 10 and figure 11, in the scenario of forced N_2 flushing with volume of 50 Liter/h and no flushing, respectively. In the arc voltage measurements the voltage induced in the measurement loop by the oscillating current is approximately 10 % of the signal.

From the enlarged view of the selected two time regions for the temporary current interruptions in figure 10: t = 901.8 µs and t = 906.4 µs, we can see that the current was temporarily interrupted, which can be identified by a short-duration rise of transient recovery voltage. After a temporary interruption of 0.2-0.3 µs, the SC switch undergoes a re-ignition, which is represented by the voltage collapse and continuation of (arc) current. After about 2 ms the current is successfully interrupted, and the voltage on the anode of the switch rises to 500 V and remains almost constant. By comparing figure 10 and figure 11 we observed that the current was interrupted 0.15 ms later without flushing than with forced N_2 flushing through the gap. Without forced flushing, the arc voltage in SC N_2 switch has a value of ≥ 100 V from 100 µs onward after the breakdown. Under situation of forced flushing the value of arc voltage is higher than that without flushing, and increases after each temporary interruption in the scenario of forced flushing. This increase might reflect the negative current-voltage characteristic of arcs in gaseous media.

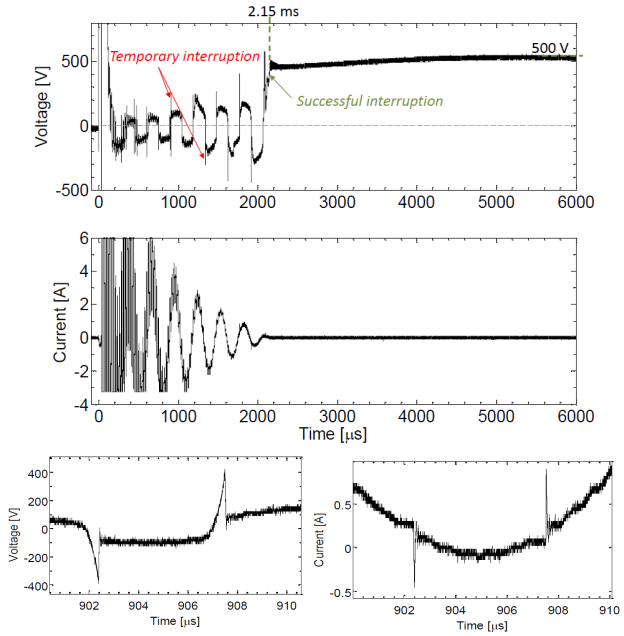

Figure 10. Voltage and current waveforms measured in SC switch in the arc interruption circuit. Pressure 50 bar, gap width 1.814 mm, L_2 = 9.8 mH, and C_2 = 1 nF. Forced N_2 flushing of about 50 Liter/h (2.73 m^3/h at STP) was supplied during the experiment.

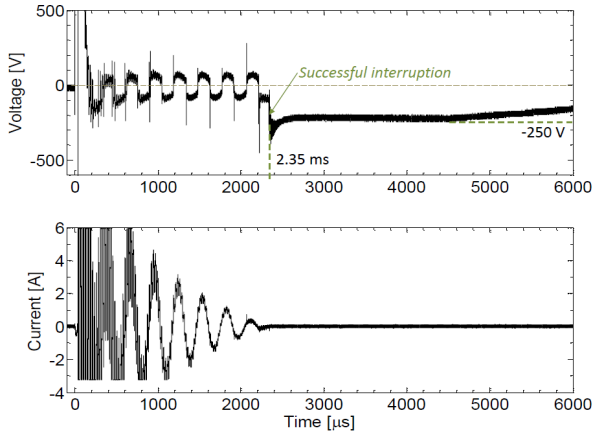

Figure 11. Voltage and current waveforms measured in the SC switch in the arc interruption circuit. Pressure 5 MPa (50 bar), gap width 1.814 mm, L_2 = 9.8 mH, and C_2 = 1 nF. No forced N_2 flushing was supplied during the experiment.

The dependence of the interruption capability on the pressure of the medium and on the flushing was investigated. The current and voltage slopes at the moment of successful arc interruption (di/dt and du/dt respectively) at the pressure of 1-4 MPa (10-40 bar) are illustrated in Figure 12. The value of the current rise slope di/dt first slightly increases with pressure, then for p > 2

MPa (>20 bar), decreases slightly with pressure, while in conventional gas media the behavior is a monotone increase with pressure. This abnormality needs more investigation. The rate-of-rise of transient recovery voltage du/dt increases with pressure, which is consistent with the observations in conventional gas media. The arc duration as a function of the pressure, under forced flushing and no flushing situation, is given in Figure 13. From the figure we can see that the current is interrupted earlier with higher pressure and under forced flushing situation. Both figure 12 and figure 13 suggest that forced flushing results in faster recovery of the former arc channel.

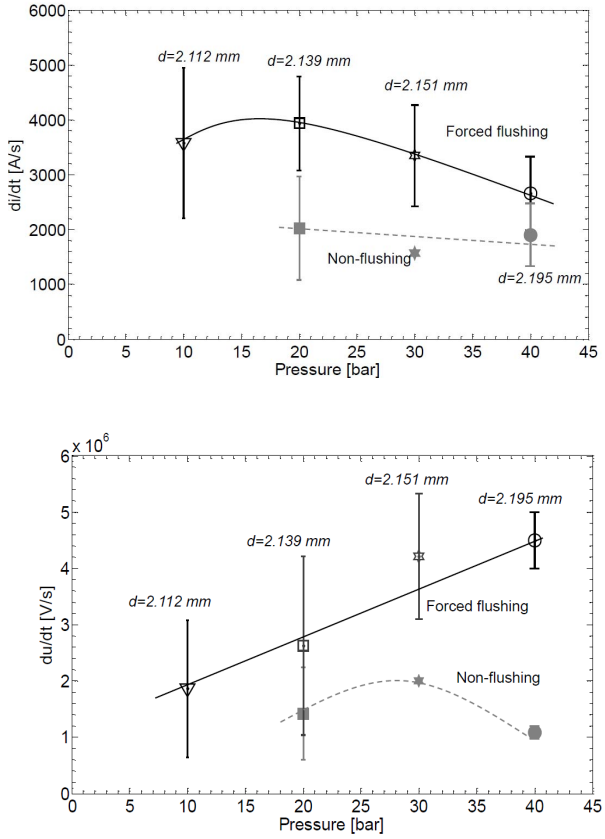

Figure 12. The rate-of-rise of current di/dt and rate-of-rise of recovery voltage du/dt at the moment of successful arc interruption in the SC switch, under situation of forced flushing and no flushing situation, at various pressures.

5 PHYSICAL MODELING

To gain insight in the mechanisms of arc development, we developed a 1D physical model of the breakdown, heating, expansion and cooling process in SCFs. The model and its details are published in [22]. In the model we simulated the streamer-to-spark transition and the discharge & post-discharge phase inside the SC N_2 breakdown. The rough time scale for physics during these processes and the temperature of neutral N_2 temperature is given in figure 14.

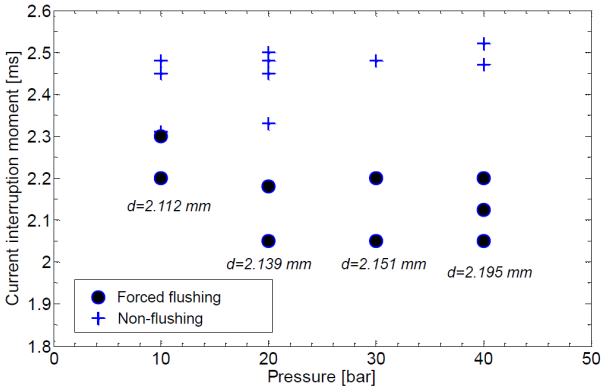

Figure 13. The arc duration under situation of forced flushing and no flushing, at various pressures.

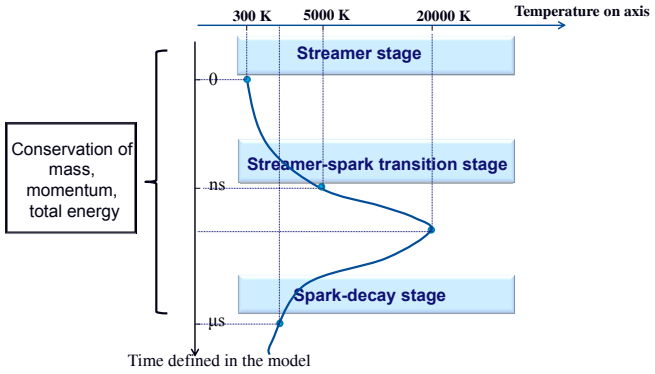

Figure 14. Simulation stages in our physical model and the estimated temperature on the axis of the spark channel in SC N_2.

The input energy for the discharge is taken from the electric field in the gap. Electrons are accelerated and collide with various gas species, thus transferring energy from the electric field to the medium. The electric field wave shape is taken from the experimental data (measured current and circuit equations). The physical equations of the model comprise the gas dynamic conservation laws plus source terms for energy input, energy storage and energy losses. The Euler equations [23–25] which cover the equations of conservation of mass, momentum, and energy are applied in the model, seen in equation (5), where ρ [kg/m^3] is the mass density, u [m/s] the velocity, p [Pa] the pressure, ε [J/m^3] the total energy density, ε_v [J/m^3] the vibrational energy density, ε_E [J/m^3] the electronically excited energy density, Q_{in} [J/m^3/s] the local power input density, Q_{out} [J/m^3/s] the local power output density, Q_R [J/m^3/s] the external discharge energy input rate, Q_{VT} [J/m^3/s] the power density relaxed from vibrational to translation energy level of N_2, and Q_{ET} [J/m^3/s] the power density relaxed from electronically excited levels as well as dissociation and ionization of N_2 molecules, η_V the fraction of the energy which goes into vibrational excited level, η_E the fraction of energy used for ionization together with the part of electronic excited energy which will not be relaxed immediately, respectively.

We assume that when the N_2 temperature in the discharge channel reaches above 5000 K, the spark channel is in local thermal equilibrium state. The model takes the results of the streamer simulation in N_2 (we scale the parameters at 0.1-8 MPa (1 bar up to 80 bar) by similarity law), and considers the energy deposition from external source, energy transfer in different energy levels, and energy loss due to different mechanisms: fluid expansion, energy relaxation from excited levels, and heat transfer. We simulate the parameters of N_2 in the spark channel till 200 µs after the streamer stage, where the temperature in the channel decays below 700 K.

$$
\begin{aligned}
&\frac{\partial \rho}{\partial t} + \frac{1}{r}\frac{\partial(\rho u r)}{\partial r} = 0 \\
&\frac{\partial(\rho u)}{\partial t} + \frac{1}{r}\frac{\partial(\rho u^2 r)}{\partial r} + \frac{\partial p}{\partial r} = 0 \\
&\frac{\partial \varepsilon}{\partial t} + \frac{1}{r}\frac{\partial(u(\varepsilon + p)r)}{\partial r} = Q_{in} + Q_{out} \\
&\frac{\partial \varepsilon_V}{\partial t} + \frac{1}{r}\frac{\partial(u\varepsilon_V r)}{\partial r} = \eta_V Q_R + Q_{VT} \\
&\frac{\partial \varepsilon_E}{\partial t} + \frac{1}{r}\frac{\partial(u\varepsilon_E r)}{\partial r} = \eta_E Q_R + Q_{ET}
\end{aligned}
\qquad (5)
$$

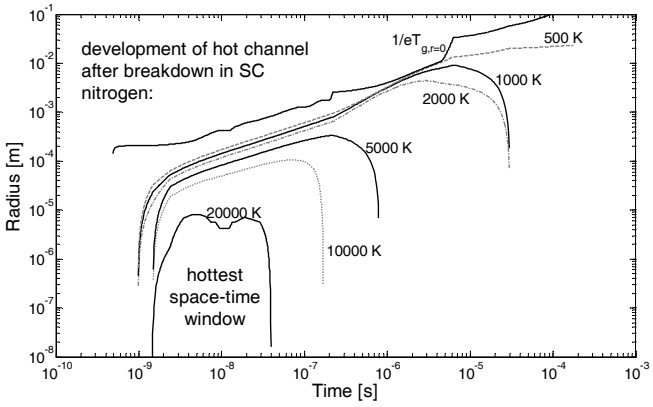

Figure 15. Space-time plot of the N_2 temperature calculated by the model. Radius of spark channel with the region defined as temperature above $1/e \cdot T_{g,r=0}$ ($T_{g,r=0}$: temperature on the axis of the spark channel), 500 K, 1000 K, 2000 K, 5000 K, 10000 K, and 20000 K and respectively.

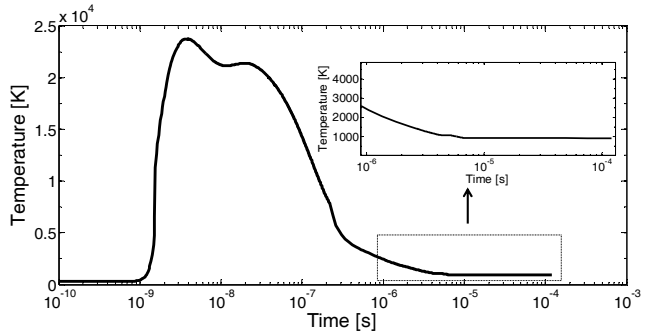

Figure 16. N_2 temperature on the axis of the spark channel with initial parameters of pd = 24 bar · mm , T_{N2} = 300 K, and d = 0.3 mm.

The simulated results for the temperature of the neutral N_2 molecule in the discharge channel as a function of time and space is depicted in figure 15. Further results of the physical model show, for SC N_2 with parameters of p = 80 bar and T = 300 K, that within nanosecond duration the spark fully develops. For a pulsed power waveform of 200 ns width it takes about 10 µs, after spark formation, for the temperature on the axis of the spark channel to decay to a value under 1500 K, seen in figure 16. We remark that these calculations only resolve the radial structure of the channel. Full 2 dimensional simulations are under way.

The dielectric recovery breakdown voltage of the SC switch gap U_{bd} is calculated with the streamer inception criterion with enhanced ionization, as been introduced in section 4.1. Three working pressures: 80 bar, 10 bar, and 5 bar are simulated. The simulated recovery breakdown voltages in N_2 at these three working pressures are given in figure 17. The simulated cold breakdown voltage has a value of 29 kV at p = 8 MPa (80 bar), d = 0.3 mm, 22 kV at p = 1 MPa (10 bar), d = 2 mm, and 11:8 kV at p = 0.5 MPa (5 bar), d = 2 mm, respectively. After the extinction of the applied energy (current lasting about 200 ns), the breakdown voltages at the three working pressures start to recover. At a time moment of 200 µs after the breakdown, the breakdown value at 8 MPa (80 bar) recovers to approximately 50 % of the cold breakdown value. The recovery breakdown voltage at p = 1 MPa (10 bar) and at p = 0.5 MPa (5 bar), however, recovers to less than 25 % of the cold breakdown voltage at the moment of 200 µs after the breakdown.

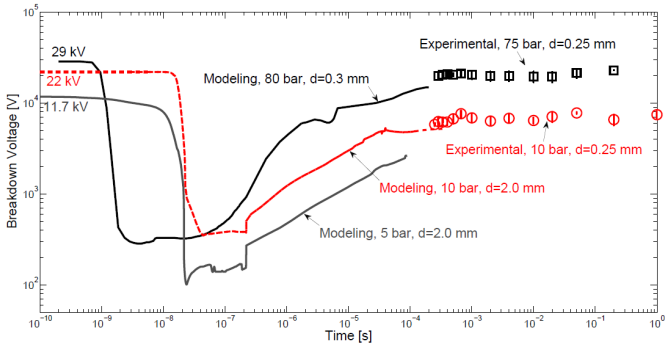

Figure 17. Comparison of the experimental and modeling results of the recovery breakdown voltage in SC N_2 switch at various N_2 pressures.

The measured recovery breakdown voltages of a SC N_2 switch at time lags between two pulses in the range of 200 µs - 1 s are also plotted in figure 17. From the figure we can find that at a similar gap width, the simulated breakdown voltages have good consistency with the experiments, though are slightly lower than the experimental measurements. The percentage of the simulated recovery breakdown voltage (at p = 80 bar, d = 0:3 mm) to the cold breakdown value at 200 µs is 50 %. The experimental results of 7.5 MPa (75 bar), 0:3 mm at 5 kHz repetition rate (time lag between pulses 200 µs) are 80 % of the value at 5 Hz. The comparison of the

simulation and experimental results of the dielectric recovery voltage in a SC N_2 switch is summarized in table 2.

Table 2. Summary of the breakdown strength and dielectric recovery in SC N_2 switches so far.

Parameter	Experimental	Calculations
Conditions	75 bar, 0.25 mm gap, transported charge 100 μC	80 bar, 0.3 mm gap, transported charge 180 μC
Recovery time after current excitation of 200 ns (no N_2 flow)	200 μs or less	200 μs
ratio U_{bd} over cold BD value	80 % after 200 μs	50 % after 200 μs
Breakdown field at low repetition rate	60 – 180 kV/mm	Paschen at high pd gives too high values; Streamer breakdown with enhanced ionization gives good fit with data

5 DISCUSSIONS AND CONCLUSIONS

Supercritical nitrogen shows excellent insulation properties and excellent recovery behavior from breakdown. Insulation strengths of 60 - 180 kV/mm were found in sub-millimeter gaps under slow and fast pulse voltages in very low repetition rate mode. These values are high compared to other insulating media. In high repetition rate mode, the recovery breakdown voltage is found to be 80 % of the cold breakdown value within 200 μs in non-flushed pre-firing mode. The interruption capability of high-frequency (≥ 7 kHz) and low (< 500 A) current of SC N_2 is investigated experimentally. The reported SC N_2 switch with fixed electrodes and small inter-electrode distance can successfully interrupt this current at approximately 2 ms after the arc initiation. The numerical model on breakdown and recovery shows recovery to 1/2 of the cold breakdown voltage within 200 μs.

The results indicate that the approach to use SCFs as switching medium in high-power applications needs further research. For the future research on the arc interruption of SCFs, moving electrode contacts and axial SCF flushing need to be considered in the new SC switch design, which can operate under high-power and power frequency experimental conditions.

ACKNOWLEDGMENT

This research is supported by the Dutch Technology Foundation STW, which is part of the Netherlands Organization for Scientific Research (NWO), and which is partly funded by the Ministry of Economic Affairs. The research is also supported by the Dutch IOP-EMVT program and by the companies Antea Group, HMVT, DNV GL, ABB and Siemens.

REFERENCES

[1] C.H. Zhang, T. Kiyan, T. Namihira, A. Uemura, S. Katsuki, H. Akiyama, T. Fang, M. Sasaki, and M. Goto, "Generation of dc corona discharge in supercritical CO_2 for environment protection purpose", IEEE Indus. Appl. Soc. (IAS) Annual Meeting in Industry Applications Conf., Vol. 3, pp. 1845–1848, 2005.

[2] M. Goto, M. Mitsugi, A. Yoshida, M. Sasaki, T. Kiyan, T. Namihira, and H. Akiyama. "Reaction of organic compound induced by pulse discharge plasma in subcritical water", J. Phys.: Conf. Series, Vol. 121, pp. 1–4, 2008.

[3] M. L. Iulia, L. L. Milton, and D. L. Edgar, "Design and optimization of a corona discharge ion source for supercritical fluid chromatography time-of-flight mass spectrometry", Analytical Chem., Vol. 68, No. 11, pp. 924–1932, 1996.

[4] H. Akiyama, T. Sakugawa, T. Namihira, K. Takaki, Y. Minamitani, and N. Shimomura, "Industrial applications of pulsed power technology", IEEE Trans. Dielectr. Electr. Insul., Vol. 14, No. 5, pp. 1051–1064, 2007.

[5] N. Budisa and D. Schulze-Makuch, "Supercritical carbon dioxide and its potential as a life-sustaining solvent in a planetary environment", Life, Vol. 4, No. 3, pp. 331–340, 2014.

[6] K. Horii, M. Kosaki, A.J. Pearmain, and A.J. McNerney, "Correlation of electrical breakdown of supercritical helium in short gaps with partial discharge in cable samples", Cryogenics, Vol. 23, No. 2, pp. 102–106, 1983.

[7] K. Nakayama and M. Tanaka, "Simulation analysis of triboplasma generation using the particle-in-cell/monte carlo collision (pic/mcc) method", J. Phys. D: Appl. Phys., Vol. 45, No. 49, pp. 495203, 2012.

[8] S. Nakayama and D. Ito, "Dc breakdown voltage characteristics in supercritical helium: breakdown in non-uniform fields", Cryogenics, Vol. 26, No. 1, pp. 12–18, 1986.

[9] T. Kiyan, M. Takade, T. Namihira, M. Hara, M. Sasaki, M. Goto, and H. Akiyama, "Polarity effect in dc breakdown voltage characteristics of pressurized carbon dioxide up to supercritical conditions", IEEE Trans. Plasma Sci., Vol. 36 No. 3, pp. 821–827, 2008.

[10] K. Yan, E.J.M. Van Heesch, A.J.M. Pemen, P.A.H.J. Huijbrechts, and Piet C.T. van der Laan, "A 10 kw high-voltage pulse generator for corona plasma generation", Rev. Sci. Instrum., Vol. 72, No. 5, pp. 2443–2447, 2001.

[11] J. Zhang, B. van Heesch, F. Beckers, T. Huiskamp, and G. Pemen, "Breakdown voltage and recovery rate estimation of a supercritical nitrogen plasma switch", IEEE Trans. Plasma Sci., Vol. 42, No. 2, No. 376–383, 2014.

[12] J.L. Hernandez-Avila, N. Bonifaci, A. Denat, and V.M. Atrazhev. Corona discharge inception as a function of pressure in gaseous and liquid nitrogen", IEEE Int'l. Sympos. Electr. Insul., pp. 493–496, 1994.

[13] A. H. Cookson, "Electrical breakdown for uniform fields in compressed gases", Proc. IEE (UK), Vol. 117, pp. 269–280, 1970.

[14] A. H. Cookson, "Review of high-voltage gas breakdown and insulators in compressed gas", Phys. Sci., Measur. Instrum., Management and Education-Reviews, IEE Proc. A, Vol. 128, No. 4, pp. 303–312, 1981.

[15] J.M.K. MacAlpine and A.H. Cookson, "Impulse breakdown of compressed gases between dielectric-covered electrodes", Proc. IEE (UK), Vol. 117, No. 3, pp. 646–652, 1970.

[16] E. Husain and R.S. Nema, "Analysis of paschen curves for air, N2 and SF6 using the Townsend breakdown equation", IEEE Trans. Electr. Insul., Vol. 17, No. 4, pp. 350–353, 1982.

[17] M. Hikita, S. Ohtsuka, N. Yokoyama, S. Okabe, and S. Kaneko, "Effect of electrode surface roughness and dielectric coating on breakdown characteristics of high pressure CO2 and N2 in a quasi-uniform electric field", IEEE Trans. Dielectr. Electr. Insul., Vol. 15, No. 1, pp. 243–250, 2008.

[18] L. Niemeyer, "A generalized approach to partial discharge modeling", IEEE Trans. Dielectr. Electr. Insul., Vol. 2, No. 4, pp. 510–528, 1995.

[19] N.H. Malik, "Streamer breakdown criterion for compressed gases", IEEE Trans. Electr. Insul., Vol. 16, No. 5, pp. 463–467, 1981.

[20] Robert C. Weast, Melvin J. Astle, and William H. Beyer, *CRC Handbook of Chemistry and Physics*, Vol. 69. CRC press Boca Raton, FL, 1988.

[21] E. H. Cohen, "The electric strength of highly compressed gases", Proceedings of the IEE-Part A: Power Engineering", Vol. 103, No. 7, pp. 57–68, 1956.
[22] J. Zhang, A.H. Markosyan, M. Seeger, E.M. van Veldhuizen, E.J.M. van Heesch and U. Ebert, "Numerical and experimental investigation of dielectric recovery in supercritical N_2", Plasma Sources Sci. Technology, Vol. 24, No. 2, 025008, 2015.
[23] N.A. Popov, "Formation and development of a leader channel in air", Plasma Phys. Reports, Vol. 29, No. 8, pp. 695–708, 2003.
[24] N.A. Popov, "Study of the formation and propagation of a leader channel in air", Plasma Phys. Reports, Vol. 35, No. 9, pp. 785–793, 2009.
[25] J. A. Riousset, V. P. Pasko, and A. Bourdon, "Air-density dependent model for analysis of air heating associated with streamers, leaders, and transient luminous events", J. Geophysical Res.: Space Phys., Vol. 115, No. A12, pp. 1978–2012, 2010.

J. (Jin) Zhang was born in Jiangsu, China, on 12 December 1985. She obtained her Bachelor of Science degree in thermal energy and dynamic engineering from Nanjing Normal University in Nanjing, China, in 2007. She graduated from RWTH-Aachen University in Aachen, Germany, as a Master of Science of electrical power engineering in 2010. In the same year, she started her Ph.D. program on exploring a new medium for high power pulse voltage switch in the Electrical Energy Systems (EES) group of the Electrical Engineering department at the Eindhoven University of Technology (TU/e), Eindhoven, the Netherlands.

E.J.M.(Bert) van Heesch was born in Utrecht, the Netherlands in 1951. He obtained a master's degree in Physics from Eindhoven University of Technology in 1975 and he has a Ph.D. in plasma physics and fusion related research from Utrecht University (1982). From 1975 till 1984 he was a researcher at the FOM-institute for Plasma Physics Rijnhuizen, the Netherlands. During 1978 he was a visiting researcher at the Fusion research facilities in Sukhumi former USSR. From 1984 till 1986 he did fusion related research at the University of Saskatchewan in Saskatoon, Canada. Since 1986 he is an assistant professor at the Eindhoven University of Technology. Here he is a key scientist in pulsed power research and pulsed plasma processing applications. He organizes projects with national and EU research agencies and industry. He is (co-) author of more than 200 international publications including more than 70 journal publications and 5 patents.

Takao Namihira was born in Shizuoka, Japan, on 23 January 1975. He received the B.S. and M.S. degrees from Kumamoto University, Kumamoto, Japan, in 1997 and 1999, respectively. Since 1999, he has been a Research Associate at Kumamoto University. He has been on sabbatical leave at the Center for Pulsed Power and Power Electronics, Texas Tech University, Lubbock.

F. J. C. M. Beckers was born in Tegelen, The Netherlands, in 1982. He received his M.Sc. degree in electrical engineering in 2008 from Eindhoven University of Technology. Since 2008 he is employed at HMVT-Oranjewoud as pulsed power engineer. In 2011 he also joined the Electrical Energy Systems group at Eindhoven University of Technology as a Ph.D. researcher. His work focuses on high power repetitive pulsed corona plasma generation for industrial scale gas-cleaning applications.

A. J. M. (Guus) Pemen was born in Breda, The Netherlands, in 1961. He received the B.Sc. degree in electrical engineering from the College of Advanced Technology, Breda, in 1986, and the Ph.D degree in electrical engineering from Eindhoven University of Technology, The Netherlands, in 2000. He worked for KEMA T\& D Power in Arnhem, The Netherlands. He joined TU/e in 1998 as assistant professor, and his research interest includes high-voltage engineering, pulsed power and pulsed plasmas. Among his achievements are the development of an on-line monitoring system for partial discharges in turbine generators and a pulsed-corona tar cracker. He is the founder of the Dutch Generator Expertise-Centre.

Aram H. Markosyan was born in Yerevan, Armenia in 1985. He obtained his M.Sc. degree in mathematics in 2008 from Yerevan State University. In late 2008 he moved to Paris and enrolled in the M.Sc. program of Mathematical Modeling, PDE and Numerical Analysis at Jacques-Louis Lions Laboratory, University Pierre and Marie Curie (UPMC, Paris 6). From 2010 to 2014 he performed Ph.D research on modeling multiple time scales in streamer discharges at Centrum Wiskunde & Informatica (CWI, Amsterdam) and obtained his degree in applied physics from Eindhoven University of Technology, The Netherlands, in 2014. He has developed the PumpKin (pathway reduction method for plasma kinetic models) open source tool freely available at www.pumpkin-tool.org. From mid. 2014, he is a research fellow in the group of Mark J. Kushner at University of Michigan, USA.

René Peter Paul Smeets has been employed at DNV GL KEMA laboratories, the Netherlands, since 1995 and is currently service area leader in testing. He received a Ph.D. de-gree for research work on distribution switchgear from Eindhoven University of Technology in 1987. Until 1995, he was an assistant professor at Eind-ho-ven Uni-versity. Dur-ing 1991 he worked with Tos-hiba Corpo-ration's Heavy App-ara-tus En-gineering Labora-tory in Japan.. In 2001, he was appointed part-time professor at the Eind-hoven University of Technology in the field of high-power switching technology and testing. He is/has been chairman and member of many working groups in the field of research and standardization in power engineering (CIGRE, IEC). He is fellow of IEEE and he is chairman of the "Current Zero Club". He published over 200 papers on high-power switching and testing in international magazines and on conferences all over the world.